Morphology and function of Neandertal and modern human ear ossicles

Alexander Stoessel[a,1], Romain David[a], Philipp Gunz[a], Tobias Schmidt[b], Fred Spoor[a,c], and Jean-Jacques Hublin[a]

[a]Department of Human Evolution, Max Planck Institute for Evolutionary Anthropology, 04103 Leipzig, Germany; [b]Department of Otorhinolaryngology, Jena University Hospital, Friedrich-Schiller-University Jena, 07743 Jena, Germany; and [c]Department of Cell and Developmental Biology, University College London, WC1E 6BT London, United Kingdom

Edited by Richard G. Klein, Stanford University, Stanford, CA, and approved August 3, 2016 (received for review April 12, 2016)

The diminutive middle ear ossicles (malleus, incus, stapes) housed in the tympanic cavity of the temporal bone play an important role in audition. The few known ossicles of Neandertals are distinctly different from those of anatomically modern humans (AMHs), despite the close relationship between both human species. Although not mutually exclusive, these differences may affect hearing capacity or could reflect covariation with the surrounding temporal bone. Until now, detailed comparisons were hampered by the small sample of Neandertal ossicles and the unavailability of methods combining analyses of ossicles with surrounding structures. Here, we present an analysis of the largest sample of Neandertal ossicles to date, including many previously unknown specimens, covering a wide geographic and temporal range. Microcomputed tomography scans and 3D geometric morphometrics were used to quantify shape and functional properties of the ossicles and the tympanic cavity and make comparisons with recent and extinct AMHs as well as African apes. We find striking morphological differences between ossicles of AMHs and Neandertals. Ossicles of both Neandertals and AMHs appear derived compared with the inferred ancestral morphology, albeit in different ways. Brain size increase evolved separately in AMHs and Neandertals, leading to differences in the tympanic cavity and, consequently, the shape and spatial configuration of the ossicles. Despite these different evolutionary trajectories, functional properties of the middle ear of AMHs and Neandertals are largely similar. The relevance of these functionally equivalent solutions is likely to conserve a similar auditory sensitivity level inherited from their last common ancestor.

middle ear | homo | 3D shape | covariation

The hominin fossil record can only provide indirect information about auditory capacities of our extinct relatives. Inferences about the evolution of the human sense of hearing require understanding of the interplay between form and function in extant species. When auditory capacities are visualized as audiograms, plotting the sensitivity for different frequencies, anatomically modern humans (AMHs) differ from the W-shaped pattern found in most anthropoid primates. AMHs are characterized by a drastically lowered high-frequency cutoff and maintaining high sensitivity in the low to midfrequencies, resulting in a U-shaped audiogram (1–7). In primates, such hearing variability is assumed to be partly related to forms of vocalization and habitat acoustics (8–10). Diverse hearing capabilities are also related to the morphology of the diminutive middle ear ossicles housed in the tympanic cavity (11, 12). The malleus, incus, and stapes form the ossicular chain that connects the tympanic membrane to the oval window of the inner ear. These bones play an important role in audition by amplifying and regulating the sound waves transmitted to the cochlea (11, 13–15). In particular, the middle ear acts as a transformer that matches the impedances between the air and the perilymph of the cochlea (16), participating in the tuning of the sensitivity levels.

Recent analyses have emphasized a distinctly derived morphology of the ossicles of AMHs compared with extant great apes (17, 18), suggesting that the ossicles of extinct hominins may provide insights into the origin of the distinct auditory capacities of AMHs.

Until recently, only a few isolated Neandertal ossicles were known, and their morphology differs consistently from AMH ossicles (19–25). Because the external acoustic meatus and cochlea have nearly identical dimensions in AMHs and Neandertals (26–28), such shape differences of the ossicles could indicate differences in auditory capacities and with it, potential implications for habitat preference and aspects of vocal communication. However, the temporal bone housing the ossicles is well-known to differentiate Neandertals from AMHs, and some of its structures express morphological covariation (29, 30). Therefore, differences in ossicle morphology between Neandertals and AMHs could also reflect variation in the spatial relationship of the ossicles within the tympanic cavity because of differences in the placement of either the oval window or the tympanic membrane (24).

Comparative and functional investigations of Neandertal ossicles were previously limited by the small sample size. High-resolution computed tomography (CT) has made it possible to study the morphology of ossicles trapped in the tympanic cavity. Here, we analyze the largest sample of Neandertal ossicles to date (22 ossicles from 14 individuals), covering a wide geographic and temporal range. We compare these fossils with Holocene and Pleistocene AMHs and African apes and investigate how previously observed ossicle characteristics fit into the Neandertal bauplan and how it evolved. Studying ossicles is methodologically challenging because of their small size and complex 3D shapes. To quantify ossicle shape, we apply a 3D geometric morphometric approach (18). We also test how differences in ossicle morphology affect the impedance matching function of the middle ear. As a functional measure, we chose an ideal transformer ratio (ITR), namely the pressure gain, which is the product of the area ratio between the tympanic membrane and stapes footplate and the lever ratio of the malleus and incus functional lengths (31–33). Finally, we analyze how ossicle shape

Significance

Middle ear ossicles are critical for audition and rarely preserved in fossils. Based on microcomputed tomography images, our comparative 3D shape analysis of Neandertal ossicles shows striking shape differences between Neandertals and anatomically modern humans (AMHs). However, these morphological differences do not affect the functional properties of the ossicles, potentially indicating consistent aspects of vocal communication in Neandertals and AMHs. Instead, a strong relationship between ossicle morphology and tympanic cavity architecture is found.

Author contributions: A.S. and J.-J.H. designed research; A.S., R.D., P.G., F.S., and J.-J.H. performed research; A.S., R.D., P.G., and T.S. analyzed data; and A.S., R.D., P.G., F.S., and J.-J.H. wrote the paper.

The authors declare no conflict of interest.

This article is a PNAS Direct Submission.

Freely available online through the PNAS open access option.

[1]To whom correspondence should be addressed. Email: alexander_stoessel@eva.mpg.de.

This article contains supporting information online at www.pnas.org/lookup/suppl/doi:10.1073/pnas.1605881113/-/DCSupplemental.

covaries with the surrounding tympanic cavity, looking into the angular orientation and distance between the tympanic sulcus and oval window as well as their respective sizes.

Results

Shape of Middle Ear Ossicles.

Malleus. In 3D shape space, Neandertals and Holocene AMHs form nonoverlapping clusters fully separated from African apes (Fig. 1*A*); means of all groups differ significantly ($P < 0.01$). Average shape distance between Holocene AMHs and Neandertals (0.120) exceeds distances between AMHs and *Pan troglodytes* (0.099) and between *P. troglodytes* and *Gorilla gorilla* (0.098). The mean shape of Pleistocene AMHs is closer to that of Neandertals (0.104) than the mean shape of Holocene AMHs. Pleistocene AMH specimens fall within the range of variation of Holocene AMHs. Compared with AMHs, Neandertals possess mallei with a shorter manubrium, a larger and more anterior–posterior flattened head, a bigger articular facet with a less developed medioinferior part, and a distinctively wide angle between the manubrium and the head (Fig. 1*D* and Tables S1 and S2).

Incus. Neandertals and AMHs form nonoverlapping clusters in 3D shape space and do not overlap with African apes (Fig. 1*B*). Mean shapes of all groups differ significantly ($P < 0.01$). Average shape distance between AMHs and Neandertals (0.128) is slightly smaller than that between AMH and *Pan* (0.136), AMH and *G. gorilla* (0.136), and between *Pan* and *G. gorilla* (0.135). Mean shape of Pleistocene AMHs is closer to that of Neandertals (0.117) than mean shape of Holocene AMHs. Pleistocene AMHs fall within the range of variation of Holocene AMHs. Compared with AMHs, Neandertals possess incudes with a shorter intercrural distance, a deeper and less symmetrical intercrural curvature, a distinctively straight long process, and a distinctively large articular facet (Fig. 1*E* and Tables S1 and S2).

Stapes. Neandertals separate from all other species, whereas AMHs overlap with *P. troglodytes* (Fig. 1*C*). Mean shapes of African apes do not differ significantly, but those of Neandertals and AMHs do ($P < 0.05$). Average shape distance between Neandertals and AMHs (0.152) is higher than that between AMHs and *P. troglodytes* (0.063). Neandertals separate from AMHs by possessing stapedes with more asymmetrical and long crura, an anterior–posteriorly shorter but inferior–superiorly broader footplate, a distinct angle between the footplate and the crura, and a head facing more anteriorly than in any other species investigated (Fig. 1*F* and Tables S1 and S2).

Ancestral State Estimation of AMH and Neandertal Ossicle Shapes.

The Euclidean distances between the estimated ancestral scores and the respective mean scores of AMHs and Neandertals in the

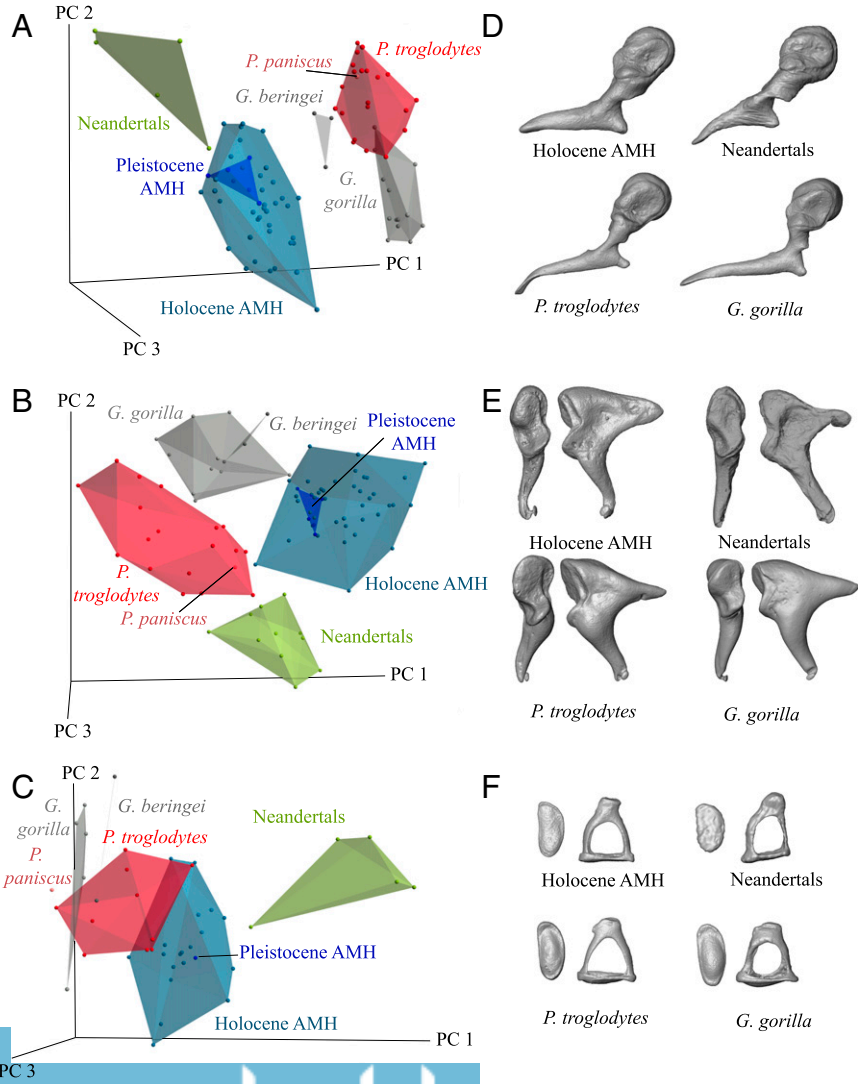

Fig. 1. Principal component (PC) analysis of the ossicle (semi)landmark sets in shape space. (*A*) Malleus. (*B*) Incus. (*C*) Stapes. Variance explained by the PCs is listed in Table S2. Mean shapes of the (*D*) malleus, (*E*) incus, and (*F*) stapes of AMHs, Neandertals, *P. troglodytes*, and *G. gorilla*. Scale has been standardized by centroid size.

space of the first three principal components show that the stapes mean shape is more derived in Neandertals than in AMHs compared with their last common ancestor (*SI Text*, *Text S1*, Fig. S1, and Table S1). Likewise, malleus and incus shape has significantly changed in both AMHs and Neandertals. Compared with the inferred morphology of the last common ancestor of *Homo* and *Pan*, the Neandertal mean shape is consistently more derived than that in AMHs (Fig. S1).

Functionally Important Factors and Ratios of the Middle Ear. All species differ significantly ($P < 0.05$) in the functional areas ratio between the areas enclosed by the tympanic sulcus and the stapes footplate and the functional lengths ratio (lever ratio) between the malleus and the incus (Fig. 2), except when comparing the functional lengths ratio ($P = 0.425$) of AMHs with that of Neandertals. All species also differ significantly ($P < 0.05$) in the ITR, an estimation of the gain in sound energy that is achieved by the middle ear, except when comparing AMHs with Neandertals ($P = 0.960$) and *P. troglodytes* with *G. gorilla* ($P = 0.480$) (Table S3).

Linking Middle Ear Morphometrics to Ossicle Shape. Compared with the African apes, AMHs and Neandertals share a smaller tympanic sulcus area and a larger middle ear length. Oval window area is less variable across the entire sample, with significant differences only between AMH and *P. troglodytes* and between *G. gorilla* and *P. troglodytes* (Tables S3 and S4). The two human groups differ significantly in the angles between the middle ear axis and the planes of the tympanic sulcus and oval window (Tables S3 and S4). Neandertals show distinctly smaller angles compared with AMHs, particular when considering the angle of the plane of the oval window and the middle ear axis. The differences in the spatial relationship between the tympanic sulcus and oval window are best visualized when looking at the oval window from a perspective parallel to the plane of the tympanic sulcus (Fig. 3). Here, the position of the oval window relative to the tympanic sulcus is more eccentrically in Neandertals. Table 1 lists middle ear parameters that explain significant amounts ($P < 0.01$) of ossicle shape. Middle ear length has the highest influence on the shape of the incus and the stapes, whereas malleus shape is most strongly affected by the area enclosed by the tympanic sulcus. Both angles, measured between the middle ear axis and the planes of the tympanic sulcus and oval window, explain a significant amount of the shape variance of each of the three ossicles.

Discussion

Our results show striking differences between Neandertal and AMH ossicles. Previously shown metric overlap of these groups (24) likely reflects allometric scaling caused by similarities in body size (34, 35). As in the skull (36, 37), the amount of shape distance between AMHs and Neandertals is comparable with (incus) or even exceeds (malleus and stapes) the distances between AMHs and African apes. Hence, just like the inner ear (38, 39), the ossicles are valuable taxonomic discriminators of late Pleistocene fossil human remains.

Despite distinct differences in ossicle morphology, functionally relevant parameters of the ossicles and the surrounding middle ear structures are largely similar between AMHs and Neandertals, particularly compared with the African apes (Fig. 2 and Tables S3 and S4). At first, this similarity seems surprising, because ossicle shape differences between AMHs and Neandertals affect the biomechanical characteristics of the ossicles when analyzed individually. Particularly, the more open angle between the manubrium and the head seen in the Neandertal malleus causes the bones' centers of mass to shift more superiorly, thereby increasing its functional length. However, we also found an increase in functional length of the incus that is of similar magnitude. Consequently, the ITR as an estimate for the impedance matching function by the middle ear is nearly identical between AMHs and Neandertals.

ITRs are simple but straightforward estimates for understanding the impedance matching function of the middle ear (33, 40). Although ITRs do not result in an accurate prediction of auditory sensitivity levels of the entire hearing range, they can be seen as an approximation for the pressure gain achieved by the middle ear at lower frequencies (33). An increase in such theoretical measures has been shown to be correlated with an increase in experimentally measured values when comparing a number of mammals (16). At higher frequencies (>10 kHz), ITRs are less reliable, because the rotational behavior of the ossicular chain becomes more complex (41, 42). The impedance matching function of the middle ear is informative about the sensitivity level but not the frequency range of hearing, because the latter depends strongly on other parameters and structures, like the cochlea (43, 44). In light of nearly identical dimensions of the external acoustic meatus and cochlea in AMHs and Neandertals (26–28), our data, thus, show no support for differences in hearing capacities between AMHs and Neandertals. This finding corroborates recent studies showing similar auditory capacities between AMHs and fossils from Atapuerca

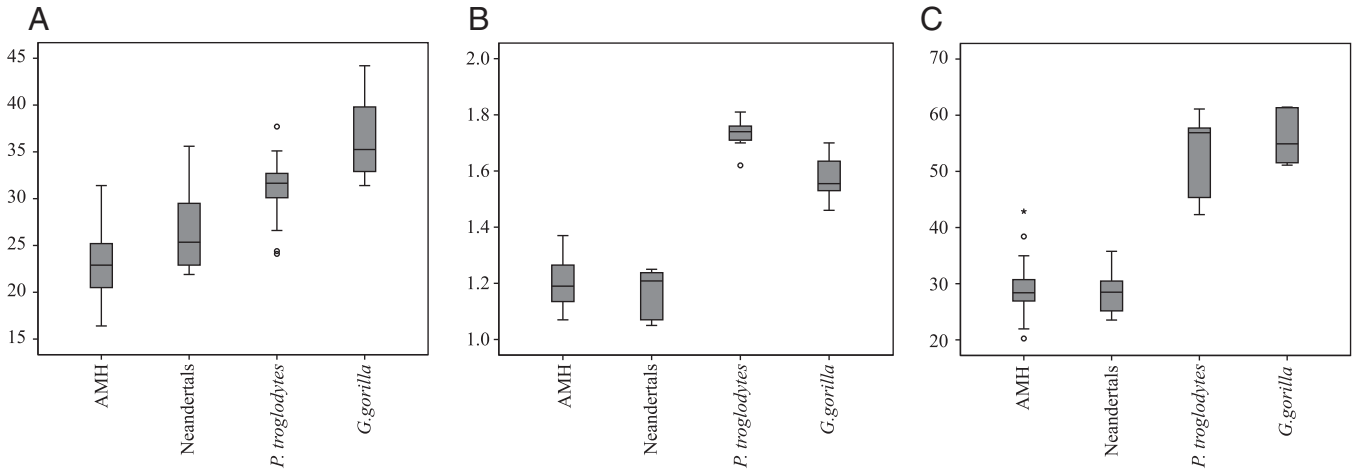

Fig. 2. Box–whiskers plots of the (*A*) functional areas ratio, (*B*) functional lengths ratio, and (*C*) ITR of AMHs, Neandertals, *P. troglodytes*, and *G. gorilla*. Sample sizes for each parameter are as follows: (*A*) AMH $n = 54$, Neandertals $n = 10$, *P. troglodytes* $n = 14$, and *G. gorilla* $n = 10$; (*B*) AMH $n = 27$, Neandertals $n = 5$, *P. troglodytes* $n = 9$, and *G. gorilla* $n = 8$; and (*C*) AMH $n = 27$, Neandertals $n = 5$, *P. troglodytes* $n = 9$, and *G. gorilla* $n = 8$.

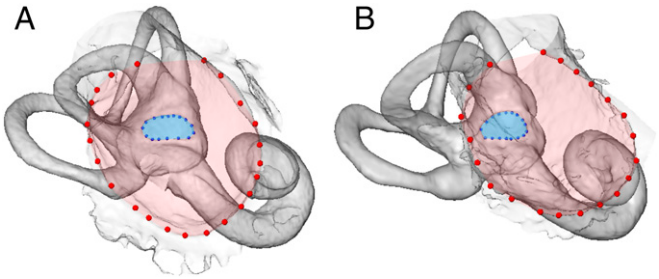

Fig. 3. Surface reconstructions of the right ear region of (*A*) an AMH (University of Leipzig Anatomy collection 58) and (*B*) a Neandertal (La Chapelle-aux-Saints 1; original left ear mirror imaged) showing the orientational/positional differences between the planes of the tympanic sulcus (red landmarks) and oval window (blue landmarks). The perspective of this view is parallel to the plane of the tympanic sulcus, and the long axis of the oval window is oriented horizontally.

(45, 46), which are considered to be close to the root of the Neandertal lineage (47). It has been shown that primate species living in different habitats (e.g., rainforest canopy and open landscapes) differ in auditory capacities, and it is likely that habitat acoustics influence vocalization and audition (8–10). Our findings, thus, potentially point to shared aspects of vocal communication in AMHs and Neandertals.

The temporal bone that houses the ear ossicles is known to discriminate between AMHs and Neandertals and among hominids in general (30, 39, 48). It has been shown that other ear structures, like the bony labyrinth, covary with changes in the surrounding temporal bone architecture (29). Our data show a number of ossicle shape changes that are correlated to variation in tympanic cavity morphology (Table 1). Different ossicle shapes might, therefore, indicate a covariation with the temporal bone. Compared with the African apes, AMHs and Neandertals share similar-sized areas enclosed by the tympanic sulcus and an increase in middle ear length. The majority of the ossicle shape aspects shared by AMHs and Neandertals are affected by changes in these linear dimensions.

The distinct ossicles shapes of Neandertals and AMHs suggest differences in their spatial relationship within the tympanic cavity (24). Those ossicle traits discriminating Neandertals from AMHs are related to variation in angular relationships between the tympanic sulcus, the oval window, and the axis of the middle ear (Table 1 and Tables S3 and S4). One of the most marked differences between Neandertals and AMHs concerns the orientation of the head of the stapes relative to its footplate. This configuration is congruent with the off-center position of the oval window relative to the tympanic sulcus in Neandertals compared with AMHs shown in Fig. 3. Our results suggest that in these hominins structural requirements of the tympanic cavity rather than functional differences drive the evolutionary shape changes in ossicle morphology. A correlation to other aspects of the surrounding morphology of the cranial base, like the glenoid fossa, tympanic area, position and orientation of the external auditory meatus, or orientation of the petrous pyramid, therefore, seems likely (30, 39, 49). Changes in cranial base morphology are thought to be associated with changes in relative brain size (50, 51). Hence, distinct differences in middle ear architecture of AMHs and Neandertals may well reflect brain expansion that occurred separately in the two lineages (52, 53).

To interpret our findings, we estimated the ancestral shape of the last common ancestor of AMHs and Neandertals using the African apes as an outgroup and computed the Euclidean distances between the AMH and Neandertal mean shapes and their estimated last common ancestor. Although the stapes seems more derived in Neandertals, the polarity of malleus and incus shape changes relative to the inferred morphology of the last common ancestor of modern humans and Neandertals remains ambiguous. However, estimation of the last common ancestor of AMHs and Neandertals does not take into account the shape variation among extinct hominins after the split from *Pan*, because only sparse and fragmentary information exists for late Pliocene *Australopithecus africanus* and early Pleistocene *Paranthropus robustus*. Findings from these fossils are interpreted as "human-like" in malleus proportions but "great ape-like" in incus and stapes dimensions (54–56). It is, therefore, more reliable to compare AMHs and Neandertal mean

Table 1. Shape changes of the malleus, incus, and stapes associated with changes in the computed middle ear parameters and shape variance explained by these middle ear parameters

Parameter	Var, %	Shape change of the ossicle when value of the parameter increases
Malleus		
i) Angle TS plane–ME axis	14*	Narrowing of angle between manubrium and head
ii) Angle OW plane–ME axis	11*	Narrowing of angle between manubrium and head
iii) TS enclosed area	20*	Increase in manubrium length
iv) OW enclosed area	3*	Decrease in manubrium curvature
v) ME length	15*	Increase in anterior–posterior flattening of head; increase in articular facet size; decrease in lateral deflection of spatula
Incus		
i) Angle TS plane–ME axis	15*	Increase of distance between long and short processes; less deeply rounded intercrural curvature; more superiorly oriented short process; more inferiorly oriented long process
ii) Angle OW plane–ME axis	11*	Increase in distance between long and short processes; less deeply rounded intercrural curvature; more superiorly oriented short but more inferiorly oriented long process
iii) TS enclosed area	12*	Decrease in short process length
iv) OW enclosed area	5*	Increase short and long process
v) ME length	21*	Increase long process length; increase asymmetry of intercrural curvature; larger articular facet; more superior oriented short crus
Stapes		
i) Angle TS plane–ME axis	12*	Decrease in stapes footplate size; longer crura; longer and more distinct head
ii) Angle OW plane–ME axis	10*	Larger long axis of footplate
iii) TS enclosed area	11*	Larger footplate; smaller head; overall broader stapes
iv) OW enclosed area	8*	Larger footplate; smaller head; overall broader stapes
v) ME length	20*	Smaller, more kidney-shaped footplate; distinct stapes head; less symmetry between crura

ME, middle ear; OW, oval window; TS, tympanic sulcus; Var, variance.
*Middle ear parameter explains a significant amount of the variance ($P < 0.01$).

shapes with the inferred last common ancestor of *Homo* and *Pan*. Here, Neandertals are consistently more derived than AMHs. This finding is concordant with genetic data that show that genes involved in skeletal morphology have changed more than previously thought in the line leading to Neandertals (57) and further adds to the distinctiveness of this archaic human species.

In conclusion, there is no evidence for differences in the auditory sensitivity level in the lower frequencies between AMHs and Neandertals. The ossicles appear to show tight covariation with the surrounding tympanic cavity. Distinctly different morphologies, likely associated with convergent brain expansion, result in similar functional properties of the middle ear of these hominin species. These functionally equivalent solutions could indicate selective pressures acting on the middle ear for conserving a similar auditory sensitivity inherited from the last common ancestor of AMHs and Neandertals and may suggest consistent aspects of vocal communication in the two species. Our findings should also be the basis for future research on the evolution of complex human spoken language.

Materials and Methods

Sample and Imaging. Tables S5 and S6 list specimens used in this study and provide information about morphological structures available for analysis. Table S7 summarizes the state of preservation of ossicles and surrounding middle ear structures in the fossil specimens. The complete fossil sample includes 16 Neandertals and 4 Pleistocene AMHs. The comparative extant sample comprises 81 mallei, 78 incudes, 37 stapedes, and 78 temporal bones, including the tympanic sulcus and oval window from AMH, *P. troglodytes*, *Pan paniscus*, *Gorilla beringei*, and *G. gorilla*. CT images of specimens housed in the American Museum of Natural History were provided by Rolf M. Quam, Binghamton University, Binghamton, NY. CT images of fossil specimens housed at the Muséum National d'Histoire Naturelle were scanned at AST-RX (Accès Scientifique à la Tomographie à Rayons X). All other specimens were scanned with the BIR ACTIS 225/300 or the Skyscan 1173 housed at the Max Planck Institute for Evolutionary Anthropology in Leipzig. Whenever possible, middle ear structures from the right side of the skull were analyzed. When necessary, left ones were mirrored. Avizo 7.1 (Visualization Science Group) was used to create 3D surface models of the ossicles and the temporal bone and place landmarks. In the case of isolated ossicles and temporal bones free of sediment, the Isosurface module was used using a single threshold value. Tympanic sulci and oval windows of sediment-filled temporals as well as ossicles scanned inside the temporal bone were isolated and visualized using the Segmentation Editor.

Ossicle Landmarks and Shape Analysis. Landmark coordinates were analyzed using Mathematica 8 (Wolfram Research, Inc.), with software routines developed by PG. The measurement protocol for ossicles is described in detail in ref. 18 and also summarized in *SI Text*, *Text S2*.

Measurement Protocol and Computation of Middle Ear Parameters. Using surface models of the temporal bone, ~25 landmarks were placed along the tympanic sulcus starting at the level of the anterior tympanic spine (slightly laterally from this point) and going in a clockwise direction when seen from medial. No landmarks were placed in the area of the tympanic notch. Along the inwardly projecting edge of the oval window, ~15 landmarks were digitized starting from its most posterior oriented protrusion and going in a clockwise direction when seen from lateral. From these landmark sets, the following parameters were computed: maximal areas enclosed by the tympanic sulcus, the oval window, and the stapes footplate; centers of maximal areas enclosed by the tympanic sulcus and the oval window; the distance between these centers (e.g., middle ear length) and the axis running through these centers (e.g., middle ear axis); and angles between tympanic sulcus and oval window planes, with the middle ear axis. Detailed formulas for these computations are provided within *SI Text*, *Text S3*. It is noted that the maximal area enclosed by the tympanic sulcus is not equal to the functional surface area of the tympanic membrane for reasons outlined in *SI Text*, *Text S3*. However, as detailed in *SI Text*, *Text S3*, we show that the maximal area enclosed by the tympanic sulcus provides an estimate for the functional area of the tympanic membrane.

To increase the sample of temporal bones, infant and juvenile (erupted M1) specimens were included. Because ontogenetic erection of the tympanic ring ends at 4–5 y in AMHs (58), values for these specimens were compared with those of adults. No difference was found for the angle between the tympanic sulcus plane and the middle ear axis (AMHs, $P = 0.522$; Neandertals, $P = 0.762$) and between the oval window plane and the middle ear axis (AMHs, $P = 0.681$; Neandertals, $P = 0.143$).

To assess whether the area enclosed by the oval window can be used to assess stapes footplate area, the ratio between these two parameters was calculated in AMH, Neandertals, *P. troglodytes*, and *G. gorilla*. On average, the stapes footplate area was found to represent 90% (±5.2%) of the area enclosed by the oval window (*SI Text*, *Text S4*)—confirming what is found in the literature (54). This value was then used to estimate stapes footplate area from oval window area.

Functional Parameters. The functional areas ratio R_Λ was computed based on the work in ref. 31:

$$R_\Lambda = \frac{\Lambda_{TS}}{\Lambda_{ST}},$$

where Λ_{TS} is the area enclosed by the tympanic sulcus, and Λ_{ST} is the area enclosed by the stapes footplate outline.

The functional lengths ratio R_{FL} was computed based on the work in ref. 11:

$$R_{FL} = \frac{FL_M}{FL_I},$$

where FL_M is the length from the malleus' center of mass (CoM) to the tip of the manubrium, and FL_I is the length from the incus' CoM to the tip of the long processus.

CoM determination was done by transforming surface mesh models into volumetric models and averaging coordinates of individual volume elements (59). Computation was done in MATLAB (The MathWorks, Inc.) using the implementation of Aitkenhead (www.mathworks.com/matlabcentral/fileexchange/27390-mesh-voxelisation).

Comparing estimated middle ear impedance function of fossil Neandertals with extant species was done using a simple ideal transformer ratio (*ITR*) (31, 33):

$$ITR = R_\Lambda \cdot R_{FL}.$$

Statistics. Permutation tests based on Procrustes distance between group means were used to test statistical significance of mean shape differences between groups (60). To this end, we compared the Procrustes distance between two group means, with average differences computed after randomly reshuffling group affiliations 10,000 times (61). To assess the influence of the morphology of the tympanic cavity on ossicle shape, we performed a multivariate regression of the Procrustes shape coordinates on each of the middle ear parameters that we have computed. Statistical significance of these correlations was tested using a permutation test based on the explained variance of the regression. Mann–Whitney–Wilcoxon tests were used in R, version 3.1.0 (The R Foundation for Statistical Computing) to assess statistical significance of interspecific differences in tympanic cavity parameters and functional ratios, ontogenetic differences in middle ear angles, and differences between stapes footplate and oval window areas (*SI Text*, *Text S4* and Table S3). Dataset S1 lists the values of the morphological and functional parameters measured in our sample.

Ancestral State Estimations. To estimate ancestral coordinates along the first three principal components describing malleus, incus, and stapes shape variation, for the successive nodes of the African hominid tree, we applied the Phylogenetic Comparative Method and particularly, the models in refs. 62–64. For AMHs and Neandertals, the mean principal component scores weighted by fossil age were used. Comparison of the Euclidean distance in the shape space of the first three principal components makes it possible to compare how each group differs from the estimated ancestral state. A detailed description of the process is provided in *SI Text*, *Text S5*.

ACKNOWLEDGMENTS. We thank A. Balzeau, I. Bechmann, C. Boesch, C. Feja, M. S. Fischer, S. Flohr, C. Funk, I. Hershkovitz, A. Hoffmann, F. Mayer, R. M. Quam, J. Radovčić, T. Schüler, J. F. Tournepiche, B. Vandermeersch, and Y. Rak for access to specimens and H. Temming and D. Plotzki for scanning. This research was funded by the Max Planck Society.

1. Coleman MN (2009) What do primates hear? A meta-analysis of all known nonhuman primate behavioral audiograms. *Int J Primatol* 30(1):55–91.
2. Elder JH (1934) Auditory acuity of the chimpanzee. *J Comp Psychol* 17(2):157–183.
3. Elder JH (1935) The upper limit of hearing in chimpanzee. *Am J Physiol* 112(1):109–115.
4. Heffner RS (2004) Primate hearing from a mammalian perspective. *Anat Rec A Discov Mol Cell Evol Biol* 281(1):1111–1122.
5. Kojima S (1990) Comparison of auditory functions in the chimpanzee and human. *Folia Primatol (Basel)* 55(2):62–72.
6. Kojima S (2003) *A Search for the Origins of Human Speech: Auditory and Vocal Functions of the Chimpanzee* (Kyoto Univ Academic Press, Kyoto).
7. Quam R, et al. (2012) Studying audition in fossil hominins: A new approach to the evolution of language. *Psychology of Language*, ed Jackson M (Nova Science Publishers, Hauppauge, NY), pp 47–95.
8. Brown CH, Waser PM (1984) Hearing and communication in blue monkeys (*Cercopithecus mitis*). *Anim Behav* 32(1):66–75.
9. Brown CH, Waser PM (1988) Environmental influences on the structure of primate vocalizations. *Primate Vocal Communication*, eds Todt D, Goedeking P, Symmes D (Springer, Berlin), pp 51–66.
10. Owren MJ, Hopp SL, Sinnott JM, Petersen MR (1988) Absolute auditory thresholds in three Old World monkey species (*Cercopithecus aethiops, C. neglectus, Macaca fuscata*) and humans (*Homo sapiens*). *J Comp Psychol* 102(2):99–107.
11. Coleman MN, Colbert MW (2010) Correlations between auditory structures and hearing sensitivity in non-human primates. *J Morphol* 271(5):511–532.
12. Quam R, et al. (2015) Early hominin auditory capacities. *Sci Adv* 1(8):e1500355.
13. Coleman MN, Ross CF (2004) Primate auditory diversity and its influence on hearing performance. *Anat Rec A Discov Mol Cell Evol Biol* 281(1):1123–1137.
14. Hemilä S, Nummela S, Reuter T (1995) What middle ear parameters tell about impedance matching and high frequency hearing. *Hear Res* 85(1-2):31–44.
15. Rosowski JJ (2013) Comparative middle ear structure and function in vertebrates. *The Middle Ear*, eds Puria S, Fay RR, Popper AN (Springer, New York), pp 31–65.
16. Puria S, Peake WT, Rosowski JJ (1997) Sound-pressure measurements in the cochlear vestibule of human-cadaver ears. *J Acoust Soc Am* 101(5 Pt 1):2754–2770.
17. Quam RM, Coleman MN, Martínez I (2014) Evolution of the auditory ossicles in extant hominids: Metric variation in African apes and humans. *J Anat* 225(2):167–196.
18. Stoessel A, Gunz P, David R, Spoor F (2016) Comparative anatomy of the middle ear ossicles of extant hominids–Introducing a geometric morphometric protocol. *J Hum Evol* 91:1–25.
19. Arensburg B, Pap I, Tillier AM, Chech M (1996) The Subalyuk 2 middle ear stapes. *Int J Osteoarchaeol* 6(2):185–188.
20. Gómez-Olivencia A, Crevecoeur I, Balzeau A (2015) La Ferrassie 8 Neandertal child reloaded: New remains and re-assessment of the original collection. *J Hum Evol* 82: 107–126.
21. Lisonek P, Trinkaus E (2006) The auditory ossicles. *Early Modern Human Evolution in Central Europe: The People of Dolni Vestonice and Pavlov*, eds Trinkaus E, Svoboda J (Oxford Univ Press, Oxford), pp 153–155.
22. Maureille B (2002) A lost Neanderthal neonate found. *Nature* 419(6902):33–34.
23. Ponce de León MS, Zollikofer CP (1999) New evidence from Le Moustier 1: Computer-assisted reconstruction and morphometry of the skull. *Anat Rec* 254(4):474–489.
24. Quam R, Martínez I, Arsuaga JL (2013) Reassessment of the La Ferrassie 3 Neandertal ossicular chain. *J Hum Evol* 64(4):250–262.
25. Quam R, Rak Y (2008) Auditory ossicles from southwest Asian Mousterian sites. *J Hum Evol* 54(3):414–433.
26. Beals ME, Frayer DW, Radovčić J, Hill CA (2016) Cochlear labyrinth volume in Krapina Neandertals. *J Hum Evol* 90:176–182.
27. Braga J, et al. (2015) Disproportionate cochlear length in genus *Homo* shows a high phylogenetic signal during apes' hearing evolution. *PLoS One* 10(6):e0127780.
28. Quam RM (2006) *Temporal Bone Anatomy and the Evolution of Acoustic Capacities in Fossil Humans* (State University of New York at Binghamton Anthropology Department, Binghamton, NY).
29. Gunz P, et al. (2013) Morphological integration of the bony labyrinth and the cranial base in modern humans and Neandertals. *Europ Soc Hum Evol* 2013:104.
30. Harvati K (2003) Quantitative analysis of Neanderthal temporal bone morphology using three-dimensional geometric morphometrics. *Am J Phys Anthropol* 120(4):323–338.
31. Heldmaier G, Neuweiler G (2004) *Vergleichende Tierphysiologie* (Springer, Heidelberg).
32. Masali M, Maffei M, Borgognini Tarli S (1991) Application of a morphometric model for the reconstruction of some functional characteristics of external and middle ear in Circeo 1. *The Neandertal Skull Circeo 1—Studies and Documentation*, eds Piperno M, Scichilone G (Istituto Poligrafico e Zecca dello Stato-Libreria dello Stato, Rome), pp 321–338.
33. Mason MJ (2016) Structure and function of the mammalian middle ear. II. Inferring function from structure. *J Anat* 228(2):300–312.
34. Nummela S (1995) Scaling of the mammalian middle ear. *Hear Res* 85(1-2):18–30.
35. Ruff CB, Trinkaus E, Holliday TW (1997) Body mass and encephalization in Pleistocene Homo. *Nature* 387(6629):173–176.
36. Harvati K, Frost SR, McNulty KP (2004) Neanderthal taxonomy reconsidered: Implications of 3D primate models of intra- and interspecific differences. *Proc Natl Acad Sci USA* 101(5):1147–1152.
37. Hublin J-J (2009) Out of Africa: Modern human origins special feature: The origin of Neandertals. *Proc Natl Acad Sci USA* 106(38):16022–16027.
38. Hublin J-J, Spoor F, Braun M, Zonneveld F, Condemi S (1996) A late Neanderthal associated with Upper Palaeolithic artefacts. *Nature* 381(6579):224–226.
39. Spoor F, Hublin J-J, Braun M, Zonneveld F (2003) The bony labyrinth of Neanderthals. *J Hum Evol* 44(2):141–165.
40. Rosowski JJ, Ravicz ME, Songer JE (2006) Structures that contribute to middle-ear admittance in chinchilla. *J Comp Physiol A Neuroethol Sens Neural Behav Physiol* 192(12):1287–1311.
41. Decraemer WF, de La Rochefoucauld O, Funnell WR, Olson ES (2014) Three-dimensional vibration of the malleus and incus in the living gerbil. *J Assoc Res Otolaryngol* 15(4):483–510.
42. Puria S, Steele C (2010) Tympanic-membrane and malleus-incus-complex co-adaptations for high-frequency hearing in mammals. *Hear Res* 263(1-2):183–190.
43. Manley GA (1971) Some aspects of the evolution of hearing in vertebrates. *Nature* 230(5295):506–509.
44. Ruggero MA, Temchin AN (2002) The roles of the external, middle, and inner ears in determining the bandwidth of hearing. *Proc Natl Acad Sci USA* 99(20):13206–13210.
45. Martínez I, et al. (2004) Auditory capacities in Middle Pleistocene humans from the Sierra de Atapuerca in Spain. *Proc Natl Acad Sci USA* 101(27):9976–9981.
46. Martínez I, et al. (2013) Communicative capacities in Middle Pleistocene humans from the Sierra de Atapuerca in Spain. *Quat Int* 295:94–101.
47. Meyer M, et al. (2016) Nuclear DNA sequences from the Middle Pleistocene Sima de los Huesos hominins. *Nature* 531(7595):504–507.
48. Lockwood CA, Kimbel WH, Lynch JM (2004) Morphometrics and hominoid phylogeny: Support for a chimpanzee-human clade and differentiation among great ape subspecies. *Proc Natl Acad Sci USA* 101(13):4356–4360.
49. Trinkaus E (2002) The cranial morphology. *Portrait of the Artist as a Child. The Gravettian Human Skeleton from the Abrigo Do Lagar Velho and Its Archeological Context*, eds Zilhão J, Trinkaus E (Instituto Português de Arqueologia, Lisbon), pp 256–287.
50. Lieberman DE, Ross CF, Ravosa MJ (2000) The primate cranial base: Ontogeny, function, and integration. *Am J Phys Anthropol* 31(Suppl):117–169.
51. Spoor F (1997) Basicranial architecture and relative brain size of Sts 5 (*Australopithecus africanus*) and other Plio-Pleistocene hominids. *S Afr J Sci* 93:182–186.
52. Bastir M, et al. (2011) Evolution of the base of the brain in highly encephalized human species. *Nat Commun* 2:588.
53. Hublin JJ, Neubauer S, Gunz P (2015) Brain ontogeny and life history in Pleistocene hominins. *Philos Trans R Soc Lond B Biol Sci* 370(1663):20140062.
54. Moggi-Cecchi J, Collard M (2002) A fossil stapes from Sterkfontein, South Africa, and the hearing capabilities of early hominids. *J Hum Evol* 42(3):259–265.
55. Quam RM, et al. (2013) Early hominin auditory ossicles from South Africa. *Proc Natl Acad Sci USA* 110(22):8847–8851.
56. Rak Y, Clarke RJ (1979) Ear ossicle of *Australopithecus robustus*. *Nature* 279(5708):62–63.
57. Castellano S, et al. (2014) Patterns of coding variation in the complete exomes of three Neandertals. *Proc Natl Acad Sci USA* 111(18):6666–6671.
58. Scheuer L, Black S, Cunningham C (2000) *Developmental Juvenile Osteology* (Academic, San Diego).
59. Patil S, Ravi B (2005) Voxel-based representation, display and thickness analysis of intricate shapes. *Proceedings of the Ninth International Conference on Computer Aided Design and Computer Graphics* (IEEE Computer Society Washington, DC), pp 415–422.
60. Good P (2005) *Permutation Tests: A Practical Guide to Resampling Methods for Testing Hypotheses* (Springer, New York).
61. Mitteroecker P, Gunz P (2009) Advances in geometric morphometrics. *Evol Biol* 36(2): 235–247.
62. Garland T, Jr, Ives AR (2000) Using the past to predict the present: Confidence intervals for regression equations in phylogenetic comparative methods. *Am Nat* 155(3):346–364.
63. Rohlf FJ (2001) Comparative methods for the analysis of continuous variables: Geometric interpretations. *Evolution* 55(11):2143–2160.
64. Rohlf FJ (2006) A comment on phylogenetic correction. *Evolution* 60(7):1509–1515.
65. De Greef D, et al. (2015) Details of human middle ear morphology based on micro-CT imaging of phosphotungstic acid stained samples. *J Morphol* 276(9):1025–1046.
66. Endicott P, Ho SY, Stringer C (2010) Using genetic evidence to evaluate four palaeoanthropological hypotheses for the timing of Neanderthal and modern human origins. *J Hum Evol* 59(1):87–95.
67. Higham T, et al. (2011) Precision dating of the Palaeolithic: A new radiocarbon chronology for the Abri Pataud (France), a key Aurignacian sequence. *J Hum Evol* 61(5):549–563.
68. Valladas H, et al. (1999) TL dates for the Neanderthal site of the Amud Cave, Israel. *J Archaeol Sci* 26(3):259–268.
69. Henry-Gambier D (2002) Les fossiles de Cro-Magnon (Les Eyzies-de-Tayac, Dordogne). Nouvelles données sur leur position chronologique et leur attribution culturelle. *Bull Mém Soc Anthropol Paris* 14:89–112.
70. Blackwell B, Schwarcz HP (1986) U-series analyses of the lower travertine at Ehringsdorf, DDR. *Quat Res* 25(2):215–222.
71. Rink WJ, Schwarcz HP, Smith FH, Radovčić (1995) ESR ages for Krapina hominids. *Nature* 378(6552):24.
72. Raynal JP (1990) Essai de datation directe. *La Chapelle-aux-Saints et la Préhistoire en Corrèze*, eds Raynal JP, Pautrat Y (La Nef, Bordeaux, France), pp 43–46.
73. Higham T, et al. (2014) The timing and spatiotemporal patterning of Neanderthal disappearance. *Nature* 512(7514):306–309.
74. Soressi M, Jones HL, Rink WJ, Maureille B, Tillier AM (2007) The Pech-de-l'Azé I Neandertal child: ESR, uranium-series, and AMS 14C dating of its MTA type B context. *J Hum Evol* 52(4):455–466.
75. Bar-Yosef O (2002) The chronology of the Middle Paleolithic of the Levant. *Neandertals and Modern Humans in Western Asia*, eds Akazawa T, Aoki K, Bar-Yosef O (Plenum, New York), pp 39–56.